

# Nanostructure effect on optical properties of porous silicon

S. RAMEZANI SANI, A. MORTEZAALI, R. S. DARIANI\*, M. R. SARKARDEI  
*Department of Physics, Alzahra University, Tehran 19938, Iran*

We calculate the dielectric constants and absorption coefficient of porous silicon from the reflectance. The normal reflectance was measured at 200-3000 nm range by unpolarized light. Kramers-Kronig analysis has been taken to use reflectance data. The real part of dielectric constant,  $\epsilon_1$ , decreases with increasing porosity in visible region. However, absorption coefficient,  $\alpha$ , increases with increasing porosity in visible region. Also the void fractions were determined from effective media approximation (EMA). Our results show that maximum void fractions are in visible region and it increases with increasing porosity. A good agreement is found between EMA and Kramers-Kronig results.

(Received April 26, 2008; accepted June 30, 2008)

*Keyword:* Porous silicon, Dielectric constants, Kramers-Kronig method, Effective media approximation (EMA), Absorption coefficient.

## 1. Introduction

Most semiconductor devices proposed today use silicon as their starting material, and over the past few decades, a great deal of silicon processing knowledge has been accumulated. Silicon itself is a poor optoelectronic material. It is an indirect gap semiconductor, and so transition probabilities are  $1/100^{\text{th}}$  that of direct gap materials.

Porous silicon (PS) was discovered in the 1950's by electropolishing silicon in dilute hydrofluoric solutions. This material was found to consist of a network of pores. Firstly, PS was only used as an intermediate step in producing a dielectric for semiconductor devices: it would be oxidized and the resulting silicon dioxide would act as an insulator. PS was reported to have a visible photoluminescence in 1984, but another six years would pass before this important property was pointed out [1].

PS may provide the means to move from standard semiconductor circuits to optoelectronic circuits. Quantum efficiencies of silicon are 0.0001% in the infrared region of the spectrum. On the other hand, reports for PS indicate quantum efficiencies as high as 10% for visible light [2].

Quantum confinement model have been used to explain the properties of PS, but some evidence suggests that the luminescence properties of PS may not simply be due to quantum confinement effects. PS is a relatively simple material to fabricate, and the raw materials are fairly inexpensive. Although PS is easy to produce, the morphology of a given PS sample is a function of the doping levels of the starting silicon and the conditions under which the etching occurs. A greater understanding of these interactions is necessary before any devices can be commercially produced [3].

However, the effects of the pore morphology on the optical properties are not well understood. Extensive experimental studies have shown that the observed optical properties depend not only on the porosity but also on the

way the PS sample is prepared. The preparation procedure modifies the morphology of PS, i. e., sizes, shapes, and interconnection of silicon quantum wires, which form PS. One of the successful model in the calculation of the electronic structure of small Si nanocrystallites is effective media approximation (EMA). EMA provides a better description of the energy-level structure of PS and is able to incorporate the interconnectivity of the system.

In this paper we apply Kramers-Kronig (K-K) analysis to calculate the optical properties of PS. Also, we investigate the nanostructure effect on optical properties of PS samples.

## 2. Kramers-Kronig analysis

There are many different methods that have been developed for the purpose of determining the optical constants of materials. Every method has differences with respect to their relative precision and the techniques with which they handle the experimental data. Depending on the experimental setup, the optical constants have been determined either only at the specified energy values or over some energy range.

Most common techniques that have been used to determine the optical constants over the whole measurement range are Kramers-Kronig analysis [4-5]. The method, in its most commonly used form, is based on the measurement of normal reflectance, over an energy range, from a bulk material and the application of an integral transformation. If the material considered is in the form of a thin film or is transparent, the application of this method becomes difficult.

We can use the imaginary part of the dielectric constant from K-K integral to find the real part [6]. Kramers-Kronig relation in integral form is

$$R_i(E) = \frac{-2E}{\pi} \int_0^{\infty} \frac{R_r(E') - R_r(E)}{E'^2 - E^2} dE' \quad (1)$$

The complex reflectance is given as

$$r(\omega) = R^{1/2}(\omega) e^{i\theta(\omega)} \quad (2)$$

Here, the  $R(\omega)$  is measured reflectance, and  $\theta(\omega)$  is phase shift arising from the reflection. If Hilbert transformation is applied to Eq. (1), the reflectance and phase shift can be related to each other as

$$\theta(E) = \frac{-E}{\pi} \int_0^{\infty} \frac{\ln R(E') - \ln R(E)}{E'^2 - E^2} dE' \quad (3)$$

In Eq. (3),  $R(E)$  is not known over the entire spectrum span, and so experimental data have been taken over a limited energy region such as  $E_1 \leq E \leq E_2$  [7]. The calculation of  $\theta(E)$  in the high energy region is usually done by power law approximation as in

$$R(E) = R(E_2) \left( \frac{E_2}{E} \right)^p, E > E_2 \quad (4)$$

where  $p$  is a power that can be obtained by numerical method [7]. On substituting equation (4) into equation (3), it can be written as

$$\begin{aligned} \theta(E) = & \frac{-E}{\pi} \int_0^{E_2} \frac{\ln R(E') - \ln R(E)}{E'^2 - E^2} dE' \\ & + \frac{1}{2\pi} \ln \left( \frac{R(E)}{R(E_2)} \right) \ln \left| \frac{E_2 + E}{E_2 - E} \right| \\ & + \frac{1}{\pi} \sum_{n=0}^{\infty} \left[ p \left( \frac{E}{E_2} \right)^{2n+1} \right] (2n+1)^{-2} \end{aligned} \quad (5)$$

the real and imaginary parts of the refractive index can be taken in terms of  $\theta(E)$  in the case of normal incidence

$$\begin{aligned} n &= \frac{1 - R}{1 + R - 2\sqrt{R} \cos(\theta)} \\ k &= \frac{2\sqrt{R} \sin(\theta)}{1 + R - 2\sqrt{R} \cos(\theta)} \end{aligned} \quad (6)$$

The dielectric constant,  $\varepsilon$ , and the absorption coefficient,  $\alpha$ , are defined as

$$\varepsilon = \varepsilon_1 + i\varepsilon_2, \varepsilon_1 = n^2 - k^2, \varepsilon_2 = 2nk \quad (7)$$

$$\alpha(E) = \frac{2E}{\hbar c} k(E) \quad (8)$$

Consequently, the optical parameters of a material were determined from the Kramers-Kronig analysis of reflectance measurements.

### 3. Experimental details

PS samples were prepared by n-type silicon wafer with (111) orientation, doped concentration of  $10^{15} \text{ cm}^{-3}$ , and  $1.5 \Omega\text{cm}$  resistivity. Ohmic contact was made on the back side samples. PS films were prepared by anodization a 40% HF – ethanol solution at a constant current density of  $25 \text{ mA/cm}^2$  for 10-20 minutes. Porosity is related to anodization time, porosity increases with increasing anodization time up to saturation stage. So, the anodization time was adjusted to obtain the desired porosity.

The morphology of the PS samples was confirmed by SEM micrographs which were obtained with a LEO 440 scanning electron microscope. The normal reflectance measurements of samples were performed by a Cary-500 Spectrophotometer in the 200-3000 nm wavelength range. Reflectance measurements have been made at room temperature and by using unpolarized light. The data taken in two nanometers intervals are transferred into a computer. For the Kramers-Kronig analysis a Fortran program has been written, and the numerical integration has been preformed.

### 4. Results and discussion

We have studied two anodization times of PS samples. Power  $p$  in Eq. (4) is calculated by using numerical method. It turned out that  $p$  is 2.2 for silicon and 1.2 for PS, which has good agreement with others [8-11].

Figure 1 shows reflectance curve for the Si sample, the PS sample for 10 min anodization, and the PS sample for 20 min anodization. The figure shows that the reflectance of PS sample decreases with increasing porosity (anodization time). This decrement is due to scattering and absorption phenomena. Absorption phenomena clearly have been shown in Fig. 3.

Fig. 2 shows real part,  $\varepsilon_1$ , and imaginary part,  $\varepsilon_2$ , of dielectric constant curves for n-type Si, PS (10 min), and PS (20 min). As we see, in visible region (1.5-3 eV)  $\varepsilon_1$  decreases with increasing porosity (anodization time). The reason could be due to decreasing transparency coefficient and increasing extinction coefficient of PS. These results have agreement with absorption coefficient curves in Fig. 3. Note that the negative real part of the dielectric function above 4 eV in Fig. 2 is in agreement with well known papers on optical properties of Si [12-14].

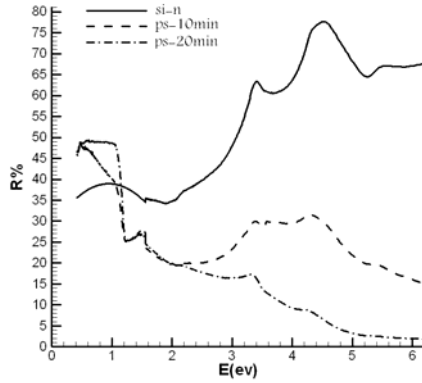


Fig. 1. Reflectance curves energy for n-type Si sample, PS sample (10 min), and PS sample (20 min).

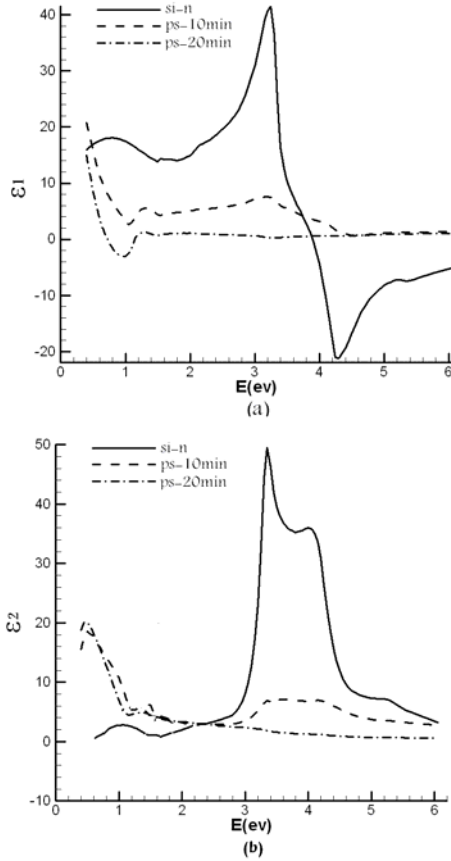


Fig. 2. The dielectric constants curve for n-type Si, PS (10 min), and PS (20 min). (a) Real part (b) Imaginary part.

Fig. 2b shows two peaks for silicon in energy region higher than 3 eV. These peaks are in  $E_1 = 3.2$  eV and  $E_2 = 4.5$  eV. They have already seen in Fig.1. These peaks are coming from bulk origin of Si and will be

disappeared by increasing the porosity [15-16]. It means that porous silicon has little bulk silicon properties and confirms PS nanostructure properties as well [17-18]. When PS has been made, its bulk properties decrease or disappear. This shows that nanostructure properties are different than bulk properties.

Fig. 3 shows absorption coefficient curves of the samples. It can be seen that in visible region (1.5-3 eV), absorption coefficient of silicon is approximately zero. It means that there is no response in visible region for Si. Also,  $\alpha$  increases with increasing porosity (anodization time) for PS.

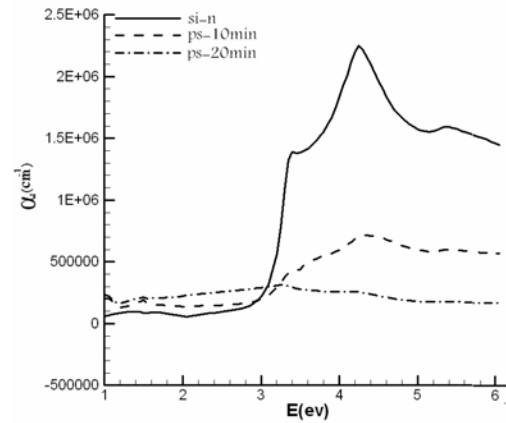


Fig. 3. Absorption coefficient curves for n-type Si, PS (10 min), and PS (20 min).

#### Effective media approximation (EMA)

We have used EMA model to find out optical properties relationship between nanostructure PS and bulk Si. Also, the results are compared with those of K-K method.

The effect of voids on optical properties of thin layers may be investigated by the Bruggman effective media approximation [19], or its modified version by Aspens et al [20].

$$\frac{\langle \epsilon \rangle - \epsilon_h}{\langle \epsilon \rangle + 2\epsilon_h} = f_v \frac{1 - \epsilon_h}{1 + 2\epsilon_h} + (1 - f_v) \frac{\epsilon - \epsilon_h}{\epsilon + 2\epsilon_h} \quad (9)$$

where  $\langle \epsilon \rangle$ , is the effective dielectric function for homogeneous material and a volume fraction of voids,  $f_v$ .

In equation (9) if we take  $\epsilon_h = \langle \epsilon \rangle$ , then we have

$$f_v \left[ \frac{1 - \epsilon_h}{1 + 2\epsilon_h} \right] = (f_v - 1) \left[ \frac{\epsilon - \epsilon_h}{\epsilon + 2\epsilon_h} \right] \quad (10)$$

where,  $\epsilon$  is complex dielectric constant for bulk silicon and  $\epsilon_h$  is complex dielectric constant for porous silicon. By using equation (10), the volume fraction of voids for

porous silicon with anodization time 10 and 20 minutes were obtained with least square approximation. The results of  $f_v$  for both PS (10 min) and PS (20 min) are given in Figure 4.

In Fig. 4,  $f_v = 0$  line represents the void fraction value for bulk silicon, positive and negative values of  $f_v$  represent layers with lower and higher densities than bulk, respectively, as explained by Aspnes et al [20]. As can be seen in Fig. 4, with increasing porosity, void fraction increases and expected layer with lower densities obtained. In visible region (0.4-0.8  $\mu\text{m}$ ), the number of voids become maximum. This shows that PS response in visible region has agreement with absorption curve in the same region which obtained by K-K analysis. In higher wavelength the numbers of voids become less and layers with higher densities obtained. Hence in the region, both absorption and conductive coefficient increase.

A result are calculated by EMA show good agreement with  $\alpha$  and  $\varepsilon_2$  curves of K-K method in the visible region.

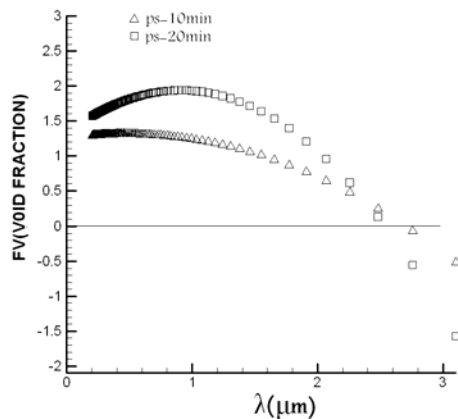


Fig. 4. Void fraction vs. wavelength for two PS samples.

## 5. Conclusions

We have studied the effect of increasing porosity (anodization time) on optical properties for n-type Si, PS (10 min), and PS (20 min). The dielectric constants and absorption coefficient were measured by Kramers-Kronig method. Kramers-Kronig analysis is still most commonly used technique in evaluating the experimental reflectance measurements.

Our results showed that in visible region (1.5 -3 eV) with increasing porosity (anodization time), transparency coefficient of PS decreased and extinction coefficient of PS increased. Two peaks are observed in  $\varepsilon_2$  - curve. They show that there is an interband transition in which the peaks disappear with increasing porosity. It means that porous silicon has not properties of bulk silicon and confirms its nanostructure properties.

Also, we investigated the agreement between K-K and EMA results for PS samples. The latter method shows that maximum concentration of voids is in visible region (1.5-3 eV). It means that, in this region, the absorption index and conductivity of samples increase. These results were also obtained from Kramers-Kronig method.

## Acknowledgement

We would like to thank Mrs. Saeideh Asghari for providing us with PS samples.

## References

- [1] L. T. Canham, Appl. Phys. Lett. **19**, 231 (1990).
- [2] P. M. Fauchet, C. C. Tsai, L. T. Canham, I. Shimizu, Y. Aoyahi, Microcrystalline semiconductors: Materials and Devices, Vol 283 (1993).
- [3] P. C. Searson, J. M. Macauley, S. M. Prokes, Journal of the Electrochemical Society **139**, 3373 (1992).
- [4] K. Yamamoto, A. Masui, Appl. Spectrosc. **49**, 639 (1995).
- [5] P. Grosse, V. Offermann, Appl. Phys A **52**, 138 (1991).
- [6] N. Peyghambarian, S. W. Koch, A. Mysyrowicz, Introduction to semiconductor optics, Prentice Hall, Englewood cliffs, 1993.
- [7] E. D. Palik, Handbook of optical constants of solid, Academic Press Inc, 1985.
- [8] D. E. Aspnes, A. Studna, Phys. Rev. **27**( 2), 985 (1983)
- [9] H. Ehrenreich, H. R. Phillipp, Phys. Rev. Lett. **8**(2), (1962).
- [10] Haziret Durmus, Haluk Satak, Haldun Karabiyik, Turk. J. Phys. **24**, 725 (2000).
- [11] D. E. Aspnes, A. A. Studna, E. K. Kingsbron, Phys. Rev. B **29**(2), 768 (1984).
- [12] S. Adachi, H. Mori, Phy. Rev. B **62**(15), 10158 (2000).
- [13] D. E. Aspese, A. A. Studna, E. Kingsbron, Phys. Rev. B **29**(2), 768 (1984).
- [14] H. Durmus, H. Safak, H. Karabiyik, Turk. J. Phys. **24**, 725 (2000).
- [15] N. K. Koshiida, et al. Appl. Phys. Lett. **63**, 2774 (1993).
- [16] L. Vina et al. Phy. Rev. B **30**, 1979 (1984).
- [17] D. P. J. Calcott, Mater. Sci. Eng. **851**, 132 (1998).
- [18] M. Cruz, M. R. Beltran, C. Wang Phys. Rev. B **59**(23), 15381 (1999).
- [19] D.A.G. Bruggeman, Ann. Phys. (Leipzig) **24**, 636 (1935)
- [20] D. E. Aspnes, E. Kingsbron, D. D. Bacon, Phys. Rev. B **21**, 3290 (1980).

\*Corresponding author: dariani@physics.queensu.ca